Structural Safety 31 (2009) 475–482

Contents lists available at ScienceDirect

Structural Safety

journal homepage: www.elsevier.com/locate/strusafe

Vulnerability-based robust design optimization of imperfect shell structures

Vissarion Papadopoulos *, Nikos D. Lagaros

Institute of Structural Analysis and Seismic Research, National Technical University of Athens, Athens 15780, Greece

ARTICLE INFO

Article history:
Received 5 June 2008
Received in revised form 29 May 2009
Accepted 30 June 2009
Available online 14 August 2009

Keywords:
Vulnerability-based robust design optimization
Non-linear TRIC shell element
Stochastic imperfections
Spectral representation
Monte Carlo simulation

ABSTRACT

A stochastic vulnerability-based robust design procedure of isotropic shell structures possessing uncertain initial geometric as well as material and thickness properties that are modeled as random fields is assessed against conventional and reliability-based robust design procedures. The main idea of the vulnerability-based design philosophy is to achieve robust optimum designs while allowing designers to determine explicitly accepted probabilities that various performance objectives will not be exceeded, by introducing additional probabilistic (vulnerability) constraints. For this purpose, a stochastic finite element methodology is incorporated into the framework of an efficient two-objective robust design optimization formulation. This combined approach is then implemented in order to obtain optimum designs of an "imperfect" shell structure involving random geometric deviations from its perfect geometry as well as a spatial variability of its modulus of elasticity and thickness. Two-objective functions, the material volume of the structure and the coefficient of variation of the buckling load of the shell, are used for the description of the optimization problem, subject to deterministic, reliability and vulnerability constraints.

1. Introduction

Deterministic formulations of structural optimization problems are not capable to reach unbiased, feasible and realistic optimum structural designs due to the fact that such formulations ignore the uncertainties involved in the various parameters affecting the structural behaviour. Once a deterministic optimum design is materialized to a real physical system, its optimal performance may vanish because of the unavoidable scattering values of the parameters, which might also be unfavorable since the performance of the "implemented" design may be far worse than expected. In practical applications, however, finding the global optimum in the presence of uncertainties in various structural parameters, such as material properties, geometric imperfections, loading variations, uncertain boundary conditions, etc., is a difficult and computationally intensive task, since for any candidate design a full stochastic analysis has to be performed for estimating various statistical quantities. Efficient methodologies are therefore required for the solution of the stochastic and the optimization part of the problem. A complete survey on these methodologies can be found in [1].

Such probabilistic optimum design formulations are usually distinguished, depending on the probabilistic system response quantities that are taken into account, in two categories: reliability-based optimization (RBO) [2–4] and robust design optimization (RDO) [5–7]. The main goal of RBO formulations is to design for safety with respect to extreme events by determining design points that are located within a range of target failure probabilities. On the other the fundamental principle of RDO is to improve product quality or stabilize performances by minimizing the effects of variations without eliminating their causes. This is usually achieved by considering the mean value and/or the standard deviation of a response quantity as an objective function and trying to establish the designs that minimize the aforementioned quantities considering deterministic or reliability constraints. Further to RDO and RBO formulations the reliability-based robust design optimization (RRDO) formulation has been addressed [8] in order to account for the influence of the probabilistic constraints in the framework of RDO of realistic structures. The recent advances in RBO, RDO and RRDO structural optimization problems can be found in the book by Tsompanakis et al. [9].

The traditional design procedures followed for imperfect shell-type structures are based on conservative corrections of deterministic non-linear analyses by means of the well-known empirical "knock-down" factors. A step forward to the aforementioned "traditional" procedure was recently achieved through accurate predictions of the scatter of the buckling loads that was accomplished via realistic descriptions of the various uncertainties involved in the problem. Such task is realizable only in the framework of stochastic finite element method (SFEM) formulations that can efficiently and accurately handle the geometric as well as physical non-linearities of shell-type structures [10–16]. This type of SFEM approaches, however, can provide with reasonable

* Corresponding author.
E-mail addresses: vpapado@central.ntua.gr (V. Papadopoulos), nlagaros@central.ntua.gr (N.D. Lagaros).

0167-4730/$ - see front matter © 2009 Elsevier Ltd. All rights reserved.
doi:10.1016/j.strusafe.2009.06.006

estimates of the scatter of the buckling loads only if the full probabilistic characteristics (marginal pdfs and correlation structures) of the involved stochastic fields are derived on the basis of corresponding experimental surveys. As this requirement is rarely satisfied, such SFEM approaches are usually implemented as "worst case" studies, based on sensitivity analyses with respect to the aforementioned parameters.

A design procedure is proposed in the present paper that addresses the vulnerability-based optimization (VBO) concept of isotropic shell structures possessing uncertain initial geometric as well as material and thickness properties that are modeled as random fields. The VBO concept used in this work is based on the trading-off performance and robustness framework that has been proposed by Mourelatos and Liang [17]. The main motivation for proposing the VBO formulation is that despite the fact that RBO and RRDO formulations lead to design points that are located within a range of target failure probabilities, intermediate (prior-to-failure) limit states possibly crucial for the structural behaviour and operational integrity are ignored. The main difference between VBO and RBO formulations is that multiple limit states are considered in VBO, apart from the failure one. Thus, VBO can be considered as an RBO procedure with multiple probabilistic constrains. The main novelty of the proposed procedure with respect to an RBO formulation with multiple probabilistic constrains, is that the definition of the multiple probabilistic constrains, named hereafter "vulnerability constrains", is associated with the classical structural vulnerability analysis. Thus, the vulnerability constraints are related to acceptable damage and/or serviceability limit states, prior and up to total structural failure, of increasing intensity.

In the present paper, the aforementioned VBO design methodology is combined with the robust design optimization leading to the vulnerability-based robust design optimization (VRDO) formulation. In VRDO, an optimum robust design is achieved while the vulnerability (probabilistic) constraints are simultaneously satisfied. This is accomplished by combining a classical vulnerability analysis in the context of a stochastic finite element method (SFEM) approach with an efficient objective robust design optimization formulation. Two-objective functions, the material volume of the structure and the coefficient of variation of the buckling load of the shell, are simultaneously used for the description of the optimization problem, while in addition to deterministic constraints, imposed by the Eurocode 3 [18], vulnerability constraints are also taken into account.

This combined approach is then implemented in order to obtain rational optimum designs of an "imperfect" isotropic shell structure involving stochastic geometric deviations from its perfect geometry as well as a spatial variability of the modulus of elasticity and the thickness of the shell. Two algorithms are employed for the solution of the two-objective optimization problem at hand; the first one is the non-domination sort evolution strategies II (NSES-II) algorithm, which is based on [19], while the second one is the Strength Pareto Evolution Strategies 2 (SPES 2) which is a variant algorithm of the one proposed in [20]. Numerical results are presented for a cylindrical panel, demonstrating the applicability of the proposed stochastic optimization methodology and the improved efficiency of the SPES 2 over the NSES-II algorithm in obtaining rational optimum designs of imperfect shell-type structures, which also satisfy the vulnerability design criteria.

2. Stochastic finite element formulation

2.1. Description of random geometric imperfections

Following an approach similar to the one described in [10], initial geometric imperfections are modeled as 2D-1V homogeneous Gaussian stochastic fields. Thus, geometric imperfections are introduced as fluctuations around a, so called, 'perfect' structural geometry as follows:

$$D(x,y) = D_0(1 + f_1(x,y)) \tag{1}$$

where D_0 is the domain of the perfect shell geometry which in this case coincides with the mean geometry of the structure and $f_1(x,y)$ is a zero mean 2D Gaussian homogeneous stochastic field. The amplitude of the imperfections is controlled by the standard deviation of the stochastic field. The coordinates x, y are the global Cartesian coordinates of the unfolded panel. Moreover, the shape of the imperfections is controlled by the correlation lengths of the stochastic field $f_1(x,y)$ in directions x and y, respectively.

It must be mentioned here that the assumption of homogeneity, although not generally applicable for the description of initial imperfections of shells, is adopted in this study and elsewhere [10,11,14] due to the fact that there is no experimental data available for this particular type of cylindrical panels. However, the proposed approach can be easily extended to non-homogeneous cases by using the spectral representation method together with an evolutionary power spectrum [11] or some other representation method such as the Karhunen–Loeve expansion [16,21]. In cases where there is lack of experimental data, a sensitivity analysis is always required with respect to various probabilistic quantities of the stochastic fields that describe the imperefections [14,16].

2.2. Non-linear finite element analysis

The finite element simulation is performed using the non-linear multilayer triangular shell element TRIC, which is based on the natural mode method. The TRIC shear-deformable facet shell element is a reliable and cost-effective element suitable for linear and non-linear analysis of thin and moderately thick isotropic as well as composite plate and shell structures. The element has 18 degrees of freedom (six per node) and hence 12 natural straining modes. Three natural axial strains and natural transverse shear strains are measured parallel to the edges of the triangle. The natural stiffness matrix is derived from the statement of variation of the strain energy with respect to the natural coordinates. The geometric stiffness is based on large deflections but small strains. The elastoplastic stiffness of the element is obtained by summing up the natural elastoplastic stiffnesses of the element layers.

The solution of the non-linear system of equations at each Monte Carlo simulation is performed using the standard incremental-iterative Newton Raphson algorithm in conjunction with the arc-length path-following technique. The effective stress for the elastoplastic analysis is computed according to the Von Mises yield criterion. Such a procedure enables the prediction of the full non-linear pre and post-buckling load–displacement path. The predicted critical buckling load is assumed to correspond to the load level at which the first negative eigenvalue of the tangent stiffness matrix of the structure appears. A detailed description of the linear elastic, geometric and elastoplastic stiffness matrix of the TRIC shell element can be found in [22–24].

2.3. Stochastic stiffness matrix

For the calculation of the stochastic stiffness matrix of TRIC the modulus of elasticity as well as the thickness of the structure are also considered in the present study as 'imperfections', in addition to geometric imperfections, due to their spatial variability. These parameters are also described as two independent 2D-1V homogeneous stochastic fields

$$\mathrm{E}(x,y) = E_0[1 + f_2(x,y)] \tag{2}$$

$$t(x,y) = t_0[1 + f_3(x,y)] \tag{3}$$

where E_0 is the mean value of the elastic modulus, t_0 is the mean thickness of the structure and $f_2(x,y)$, $f_3(x,y)$ are two zero mean 2D Gaussian homogeneous stochastic fields corresponding to the variability of the modulus of elasticity and the thickness of the shell, respectively. Stochastic fields $f_2(x,y)$ and $f_3(x,y)$ are assumed uncorrelated. The stochastic stiffness matrix of the shell element is derived using the midpoint method as this is implemented in [11,15].

The generation of sample functions for stochastic fields $f_1(x,y)$, $f_2(x,y)$ and $f_3(x,y)$ corresponding to the variations of the geometric, material and thickness imperfections, respectively, is performed using the spectral representation method [25]. The two-sided power spectral density function used for the description of the above mentioned fields is assumed to correspond to an autocorrelation function of exponential type and is given by

$$S_{f_0 f_0}(\kappa_1, \kappa_2) = \frac{\sigma_f^2}{4\pi} b_1 b_2 \exp\left[-\frac{1}{4}\left(b_1^2\kappa_1^2 + b_2^2\kappa_2^2\right)\right] \tag{4}$$

where σ_f denotes the standard deviation of the stochastic field and b_1, b_2 denote the parameters that influence the shape of the spectrum which are proportional to the correlation distances of the stochastic field along the x_1, x_2 axes, respectively, and κ_1, κ_2 are wave numbers. A large number N_{SAMP} of sample functions are produced, leading to the generation of a set of stochastic stiffness matrices while first and second order moments of the computed buckling loads are estimated by the brute-force Monte Carlo simulation.

3. Vulnerability-based robust design optimization

Vulnerability-based robust design optimization (VRDO) aims to minimize both the weight and the variance of the structural capacity when the geometric and/or material properties are considered as random, while ensuring that a series of target probabilities (vulnerability objectives) will not be exceeded. These probabilities are defined as the frequencies with which various performance parameters (for example displacements or stresses) violate increasing limit state conditions. These limit states are defined as being conditional to corresponding (predefined) increasing loading conditions (actions) with the final limit state being the structural failure. Thus, vulnerability-based design of shell structures requires the calculation of a series of limit state probabilities for a corresponding series of limit states conditioned to a given, monotonically increasing, sequence of loads.

A general formulation of the VRDO problem can be stated as a multi-objective problem as

$$\begin{aligned}
&\min_{\mathbf{s}\in\mathbf{F}} \quad f = [C(\mathbf{s},\boldsymbol{\mu}(\mathbf{X})), \mathbf{COV}_{\mathrm{resp}}(\mathbf{s},\boldsymbol{\mu}(\mathbf{X}))]^{\mathrm{T}} \\
&\text{subject to} \\
&\text{(a)} \quad \text{deterministic constraints}: \\
&\qquad g_j(\mathbf{s},\boldsymbol{\mu}(\mathbf{X})) \leqslant 0 \quad j = 1,\ldots,k \\
&\text{(b)vulnerability constraints}: \\
&\qquad p_i[v(\mathbf{s},\boldsymbol{\mu}(\mathbf{X})) > v_i|_{P=P_i}] \leqslant p_{i,\mathrm{target}} \quad i = 1,\ldots,m
\end{aligned} \tag{5}$$

where f are the objective functions related to the material cost C and the vector that contains the coefficient of variation of selected response quantities $\boldsymbol{COV}_{\mathrm{resp}}$. In many structural design problems the main objective is to find economical designs, this is the reason for choosing the material cost C as the first objective to minimize. It is important, thought, to fulfill structural performance constraints in a probabilistic environment; for this reason $\boldsymbol{COV}_{\mathrm{resp}}$ is selected as the second objective to be minimized. Vector $\mathbf{s}$ represents the design variable vectors, and $\boldsymbol{\mu}(\mathrm{X})$ represents the vector of the random field used for the description of the uncertain parameters involved in the problem, which is a function of the position vector $\mathbf{X}$. F is the feasible region where all the deterministic constraint functions g_j are satisfied while the maximum conditional probability $p_i\left[v(\mathbf{s},\boldsymbol{\mu}(\mathbf{X})) > v_i|_{P=P_i}\right]$ that the performance variables $v(\mathbf{s},\boldsymbol{\mu}(\mathrm{X}))$ (for example displacements and/or stresses) are greater than the desired design levels v_i, given that the load level is P_i, does not exceed a predefined target probability $p_{i,\mathrm{target}}$.

With reference to Eq. (5), the step of minimizing the objective function with respect to the deterministic constrains is the part of the RDO, which is an integral part of the VRDO procedure. In addition, the mth limit state in Eq. (5) corresponds to structural failure and for this limit state the vulnerability constraint is equivalent to the classical reliability constraint $p_f(\mathbf{s},\boldsymbol{\mu}(\mathbf{X})) \leqslant p_{f,\mathrm{target}}$, p_f being the probability of structural failure. Therefore, the final (ultimate) limit state for the VRDO procedure coincides with the conventional structural reliability criterion (probability of structural failure), as this is defined in a RRDO formulation. Thus, the VRDO may be seen as a generalization of the RRDO methodology with multiple probabilistic constraints associated with various prior-to-failure structural performance levels. If only the final probabilistic constrain is considered, then the VRDO reduces to a RRDO procedure. Similar to the RRDO, the basic philosophy of VRDO consists in allowing designers to determine explicitly accepted probabilities that various performance objectives will not be exceeded, by introducing additional probabilistic (vulnerability) design checks. A comparison between conventional RDO, RRDO and VRDO, both in terms of their specific formulations as well in terms of the optimum results that they produce, will be given in detail through an example in Section 5.

4. Solving the multi-objective optimization problem

Several methods have been proposed in the past for treating structural multi-objective optimization problems [26,27]. In this work two algorithms are used in order to handle the two-objective optimization problem at hand. The first one is based on the non-domination sort genetic algorithm II (NSGA-II) developed by Deb et al. [19] while the second one is based on the strength Pareto evolutionary algorithm 2 (SPEA 2) developed by Zitzler et al. [20]. The evolution strategies (ES) method has been proved very efficient for solving single objective structural optimization problems [28,29]. In both basic algorithms this is the reason for being combined with the philosophies of the two multi-objective optimization methods. The resulting multi-objective optimization algorithm are denoted as NSES-II(μ + /,λ) and SPES 2(μ + /,λ).

4.1. Non-dominated sorting evolution strategies (NSES-II)

The main part of the NSES-II algorithm is the fast-non-domination-sort procedure according to which a population is sorted in non-dominated fronts and it is based on the work by Deb et al. [19]. This algorithm identifies non-dominated individuals in the population, at each generation, to form Pareto fronts, based on the concept of non-dominance. After this, the basic operators of ES are performed. In the ranking procedure, the non-dominated individuals in the current population are first identified. Then, these individuals are assumed to constitute the first non-dominated front with a large dummy fitness value. All these solutions have an equal reproductive potential. In order to maintain population diversity, these non-dominated solutions are then shared with their dummy fitness value. Afterward, the individuals of the first front are ignored temporarily, and the rest of the population is processed in the same way to identify individuals for the second non-dominated front. They are assigned a dummy fitness value, which is a little smaller than the worst shared fitness value observed in the solutions of the first non-dominated front. This process continues until the whole population is classified into non-dominated

fronts. Since the non-dominated fronts are defined, the population is then reproduced according to the dummy fitness value.

4.2. Strength Pareto evolution strategies (SPES 2)

The basic option of SPES 2($\mu + /, \lambda$) algorithm was proposed in [20] as an approach that incorporates several of the desirable features of other well-known multi-objective evolutionary algorithms. SPES 2($\mu + /, \lambda$) implements elitism through the maintenance of an external set of best solutions found during the whole iteration loop. Elitism, when applied by an evolutionary algorithm, guarantees that the solutions with higher fitness will not be eliminated during the run of the optimization algorithm. The non-dominated solutions in the external set are used to determine the fitness of the current population (set of solutions) and also take part in the selection process for reproduction. In SPES 2($\mu + /, \lambda$), the fitness of a solution in the population depends on the best solutions in the external set but is independent of the number of solutions this solution dominates, or is dominated by, within the population. The most important aspects of this algorithm are the fitness assignments and the clustering procedure. In each iteration, a population of individuals $\mathbf{B}_p^{(g)}$ is obtained, and the non-dominated solutions of this population are copied in $\mathbf{A}^{(g)}$ (external population). Next, the solutions of $\mathbf{A}^{(g)}$ that are dominated by other solutions are eliminated, obtaining the front of Pareto of $\mathbf{A}^{(g)}$. In SPES 2($\mu + /, \lambda$), the number of externally stored non-dominated solutions is limited to λ. If the number of solutions of the Pareto front is greater than λ, it is necessary to reduce the external population by some means of clustering.

5. Numerical results

The hinged isotropic cylindrical panel of Fig. 1 is considered in order to illustrate the efficiency of the proposed vulnerability-based robust design optimization formulation having both sizing and shape design variables. The loading, the length L in both directions as well as the mean material properties of the perfect shell is also shown in Fig. 1. Considering the geometric properties of the shell, only the length L is considered as constant during the optimization procedure, while the mean thickness t_0 of the panel and the angle θ are considered as design variables subjected to the constraints $4^\circ \leqslant \theta \leqslant 8^\circ$ and 2 mm $\leqslant t_0 \leqslant$ 6 mm. The curve edge nodes of the panel are assumed to be free in all directions while the nodes along the sides are hinged (fixed against translation only). The material is considered to be elastic-perfectly plastic.

The geometrically non-linear elastic as well as elastoplastic response of point A of the perfect cylinder with respect to the applied vertical load P, is shown in Fig. 2 for the mean values of the design parameters, i.e., $\theta = 6$ and $t_0 = 4$ mm. The cylindrical panel is discretized with a 21×21 mesh of 400 TRIC shell elements. A mesh convergence study for this particular example is presented in a

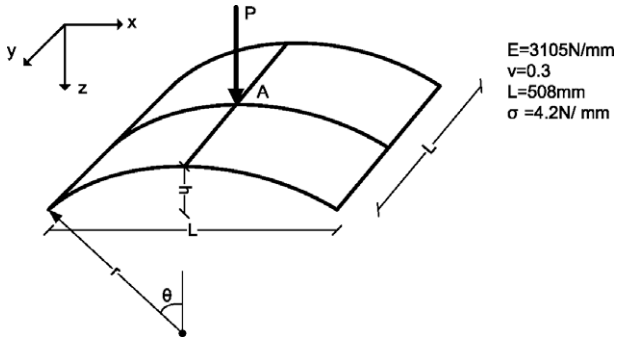

Fig. 1. Geometry, and material data of the cylindrical panel.

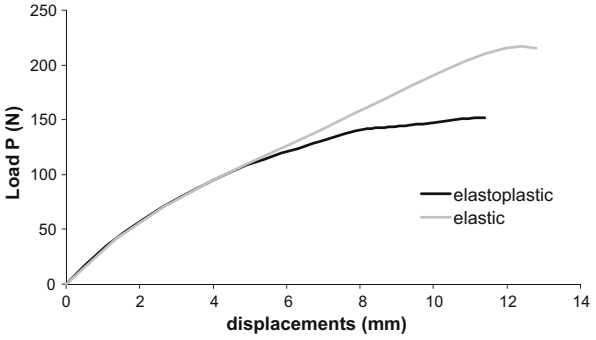

Fig. 2. Central load–displacement curve of the perfect cylindrical panel ($t = 6$ mm, $\theta = 6^\circ$).

previous investigation [10] where the computational efficiency of the TRIC element in non-linear shell analysis was demonstrated. For the discretization of the stochastic fields, the same mesh used for the finite element analysis is implemented since it is a fraction of the correlation length parameters adopted in this example [10]. The ultimate load of the perfect configuration is found to be $P_u = 217$ N for the elastic shell and $P_u = 152$ N for the elastoplastic.

5.1. Parametric study

A parametric study is performed with respect to the correlation lengths of the stochastic fields modeling the geometric material and thickness imperfections in x, y directions, since no experimental data of initial imperfections is available for this specific type of structure. This parametric study is performed for the cylindrical panel possessing the mean values of the design parameters, i.e., angle $\theta = 6^\circ$ and thickness $t_0 = 4$ mm. Two dimensional (2D) stochastic imperfections were considered in order to investigate their effect on the buckling load using an alternative version of Eq. (1)

$$r(x,y) = r_0(1 + f_1(x,y)) \tag{6}$$

where r_0 is the radius of the perfect geometry. For all cases, the standard deviation σ_f of the stochastic field $f_1(x,y)$ of the initial geometric imperfections is assumed to be $\sigma_f = 0.0001\ r_0$. This value for the standard deviation corresponds to a deviation of the nodal coordinates with respect to the perfect geometry of the order of 5% of the shell thickness. For the material and thickness imperfections the standard deviation was assumed to be $\sigma_f = 0.1\ E_0$ and $\sigma_f = 0.1\ t_0$, respectively.

Fig. 3 presents the mean value and coefficient of variation (COV) of the buckling load considering initial geometric imperfections as a standalone case, as a function of the correlation length parameter $b = b_1 = b_2$ used for the definition of the power spectrum of Eq. (4).

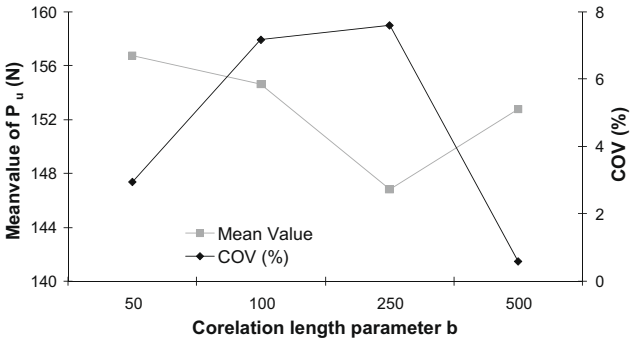

Fig. 3. Mean value and coefficient of variation COV (%) of the ultimate load P_u as a function of the correlation length parameter b for 2D variation of initial geometric imperfections.

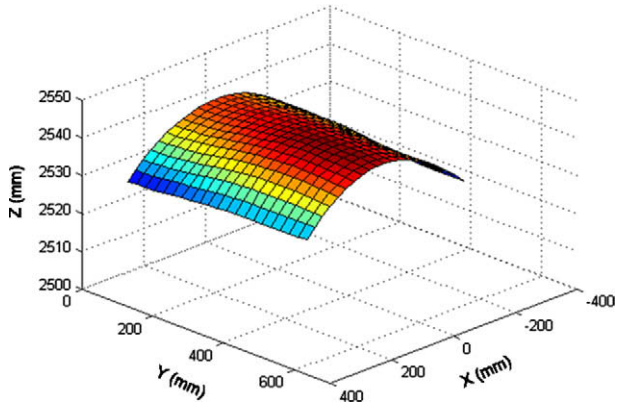

Fig. 4. One sample function of 2D random initial geometric imperfections for $\sigma_f = 0.10$ and $b = 250$ ($t = 6$ mm, $\theta = 6°$).

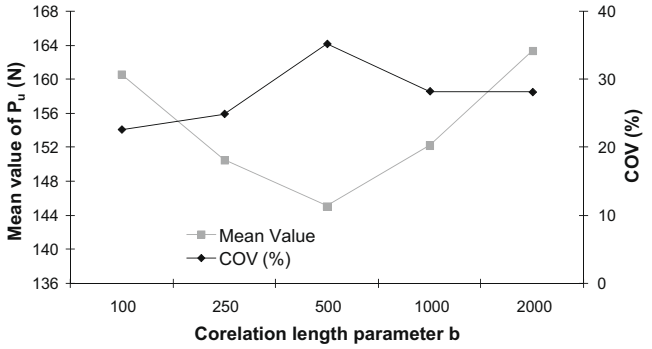

Fig. 5. Mean value and coefficient of variation COV (%) of the ultimate load P_u as a function of the correlation length parameter b for 2D variation of material and thickness imperfections, combined with geometric imperfections with $b = 250$.

It can be observed from Fig. 3 that the lowest mean value and the largest COV correspond to the same correlation length parameter $b = 250$. The mean value and the COV of P_u for this value of b is found to be 147 N and 7.6%, respectively. Using now this value of $b = 250$ as fixed, the previous parametric study is repeated considering the combined effect of geometric material and thickness imperfections. In Fig. 4 one sample function, generated using the aforementioned correlation parameter $b = 250$, is presented.

Fig. 5 presents the mean value and coefficient of variation of the buckling loads as a function of the correlation length parameter b used for the modeling of the modulus of elasticity and thickness according to Eqs. (2) and (3). From this figure it can be observed that the lowest mean value and the largest COV correspond to the same correlation length parameter $b = 500$. The mean value and the COV of P_u for this value of b is found to be 145 N and 35.3%, respectively. From the comparison of Figs. 3 and 5 it can be seen that the incorporation of the material and thickness imperfections to the model of the initial geometric imperfections results in a significant increase of the COV, while the mean value of P_u remains almost constant. Therefore, the "worst" imperfection mode for this case corresponds to a correlation length parameter $b_1 = b_2 = 250$ for the initial geometric imperfections and $b_1 = b_2 = 500$ values for the random material and thickness imperfections. These values were assumed fixed for the subsequent optimization procedure.

5.2. Solving the optimization problem

In the second part of this study, the RDO, RRDO and VRDO problems are considered and the efficiency of the NSES-II($\mu + \lambda$) and SPES 2($\mu + \lambda$) algorithms is studied. All three formulations are defined as a two-objective optimization problem where the material volume and the coefficient of variation of the buckling load are to be minimized, while the critical correlation lengths derived from the previously described parametric study. The formulation of the RDO problem is defined as

$$\begin{aligned} \min_{\mathbf{s}\in\mathbf{F}} \quad & [\mathrm{VOL}(\mathbf{s}, \boldsymbol{\mu}(x,y)), \mathrm{COV}_P(\mathbf{s}, \boldsymbol{\mu}(x,y))]^{\mathrm{T}} \\ & \mathbf{s} = [\theta, t_0]^{\mathrm{T}} \\ \text{subject to} \quad & \left.\begin{array}{l} 4^\circ \leqslant \theta \leqslant 8^\circ \\ 2\ \mathrm{mm} \leqslant t_0 \leqslant 6\ \mathrm{mm} \end{array}\right\} \text{bounds of the design variables} \\ & \sigma_{\text{von Mises}} \leqslant \sigma_y/1.10, \sigma_y = 4.2\ \mathrm{N/mm^2} \end{aligned} \tag{7}$$

where the material volume (VOL) of the structure and the coefficient of variation of the buckling load (COVP) constitute the two objectives of the problem. Using the $\mathrm{COV_P}$, a combined criterion is applied taking into account simultaneously the effect of both the mean and the standard deviation of the shell buckling load. Essentially we are seeking for a maximum mean buckling load with a simultaneous minimum standard deviation. The von Mises yield criterion is employed in order to assess deterministically the value of an equivalent stress that will be compared with the yield stress σ_y. Therefore the following expression has to be satisfied for each triangular shell element

$$\sigma_{\text{von Mises}} = \sqrt{\sigma_1^2 + \sigma_2^2 - 3\sigma_1\sigma_2 + 3\tau^2} \leqslant \sigma_y/\gamma_{M0} \tag{8}$$

where σ_1, σ_2, τ are the stresses in the middle surface of the triangle and γ_{M0} is a safety factor equal to 1.10, according to Eurocode 3 [18]. The design loads considered for this check are the shell self-weight, 10 N/m^2 permanent load and 15 N/m^2 live load.

Considering now the RRDO problem, this defined as follows:

$$\begin{aligned} \min_{\mathbf{s}\in\mathbf{F}} \quad & [\mathrm{VOL}(\mathbf{s}, \boldsymbol{\mu}(x,y)), \mathrm{COV}_P(\mathbf{s}, \boldsymbol{\mu}(x,y))]^{\mathrm{T}} \\ & \mathbf{s} = [\theta, t_0]^{\mathrm{T}} \\ \text{subject to} \quad & \left.\begin{array}{l} 4^\circ \leqslant \theta \leqslant 8^\circ \\ 2\ \mathrm{mm} \leqslant t_0 \leqslant 6\ \mathrm{mm} \end{array}\right\} \text{bounds of the design variables} \\ & \sigma_{\text{von Mises}} \leqslant \sigma_y/1.10, \sigma_y = 4.2\ \mathrm{N/mm^2} \\ & p(P_u < 50\ \mathrm{N}) \leqslant 1.0\% \end{aligned} \tag{9}$$

where the reliability constraint imposed is defined as the probability that the buckling load is less than 50 N not to be greater than 1.0%.

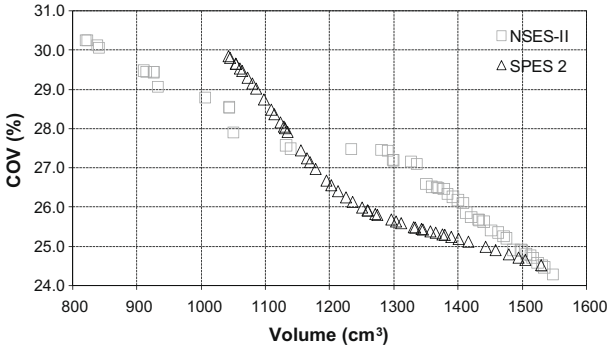

Fig. 6. Comparison of Pareto front curves obtained after 15 generations with the NSES-II(50 + 50) and SPES 2(50 + 50) optimization schemes.

Finally, the VRDO formulation is defined as follows:

$$
\begin{aligned}
\min_{\mathbf{s}\in\mathbf{F}} \quad & [\mathrm{VOL}(\mathbf{s}, \boldsymbol{\mu}(x,y)), \mathrm{COV}_P(\mathbf{s}, \boldsymbol{\mu}(x,y))]^{\mathrm{T}} \\
& \mathbf{s} = [\theta, t_0]^{\mathrm{T}} \\
\text{subject to} \quad & \left.\begin{array}{l} 4^{\circ} \leqslant \theta \leqslant 8^{\circ} \\ 2\ \mathrm{mm} \leqslant t_0 \leqslant 6\ \mathrm{mm} \end{array}\right\} \text{bounds of the design variables} \\
& \sigma_{\text{von Mises}} \leqslant \sigma_y/1.10, \quad \sigma_y = 4.2\ \mathrm{N/mm^2} \\
& p(u_A > 4\ \mathrm{mm}|_{P=30\ \mathrm{N}}) \leqslant 5.0\% \\
& p(u_A > 6\ \mathrm{mm}|_{P=40\ \mathrm{N}}) \leqslant 3.0\% \\
& p(P_u < 50\ \mathrm{N}) \leqslant 1.0\%
\end{aligned} \tag{10}
$$

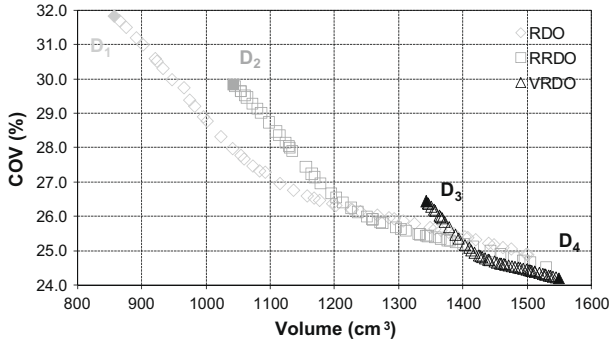

Fig. 7. Pareto front curves for the RDO, RRDO and VRDO formulations, all obtained after 15 generations with the SPES 2(50 + 50) optimization scheme.

Table 1
Formulations of the optimization problem – a comparative study.

Design	Design (angle θ, mean thickness $\bar{t}$)	Volume (cm^3)	COV (%)
D1	4.00°, 3.32 mm	857	32.43
D2	4.09°, 4.04 mm	1043	30.98
D3	4.00°, 5.19 mm	1342	27.23
D4	4.16°, 6.00 mm	1549	25.18

where the two additional vulnerability constraints are defined with reference to a performance variable assumed to be the vertical displacement of node A. These additional probabilistic constraints enforce the condition that the probability that u_A is greater than 4 and 6 mm, under the condition that the vertical load P is equal to 30 and 40 N, is less than the target levels of 5% and 3%, respectively. These additional probabilistic constraints are assumed to correspond to prior-to-failure acceptable serviceability levels of the shell structure. In Eqs. (7), (9) and (10), $\boldsymbol{\mu}(x,y)$ denotes the vector of the random fields involved in the problem given by

$$\boldsymbol{\mu}(x,y) = [f_1(x,y)\, f_2(x,y)\, f_3(x,y)]^T \tag{11}$$

where $f_1(x,y)$, $f_2(x,y)$, $f_3(x,y)$ are the random fields of Eqs. (1)–(3), respectively. In all cases considered, the probabilities of exceedance are estimated using a brute-force MCS with $N_{\mathrm{SAMP}} = 1000$.

In order to define the optimization scheme that combines computational efficiency and robustness the Pareto fronts after 15 generations obtained with NSES-II(50 + 50) and SPES 2(50 + 50) optimization schemes are compared (see Fig. 6) corresponding to the solution of the RRDO optimization problem of Eq. (9). It can be seen that for the problem at hand the optimization scheme SPES 2(50 + 50) outperforms NSES-II(50 + 50) obtaining a better quality Pareto front. Thus, for all test cases examined, the SPES 2(50 + 50) optimization scheme is employed. The corresponding three Pareto front curves obtained with the SPES 2(50 + 50) optimization scheme for the three formulations (RDO, RRDO and VRDO) are shown in Fig. 7.

In order to examine the variability of the designs composing the three Pareto front curves obtained from the formulations of Eqs. (7), (9) and (10), four designs are selected from the three front curves, as shown in Fig. 7, in order to be compared with respect to the mean value and COV of the buckling load along with probability of violation. Three of these designs, i.e., designs D1, D2 and D3, correspond to the one extreme end of the three Pareto front curves where the material volume is the dominant criterion, while design D4 corresponds to the optimum design obtained if the coefficient of variation of the buckling load is the dominant criterion. The four designs, along with the material volume, the coefficient

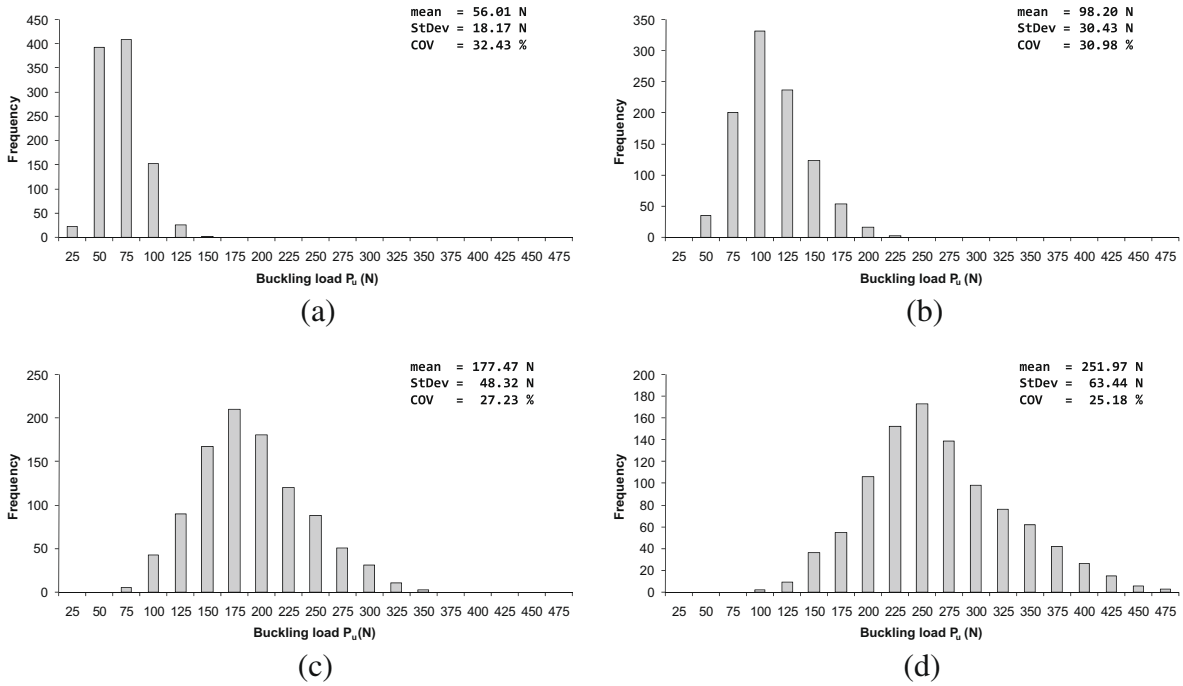

Fig. 8. Histograms of the buckling load factor P_u for the four designs (a) D1, (b) D2, (c) D3 and (d) D4 with the combined geometrical, material and thickness imperfections.

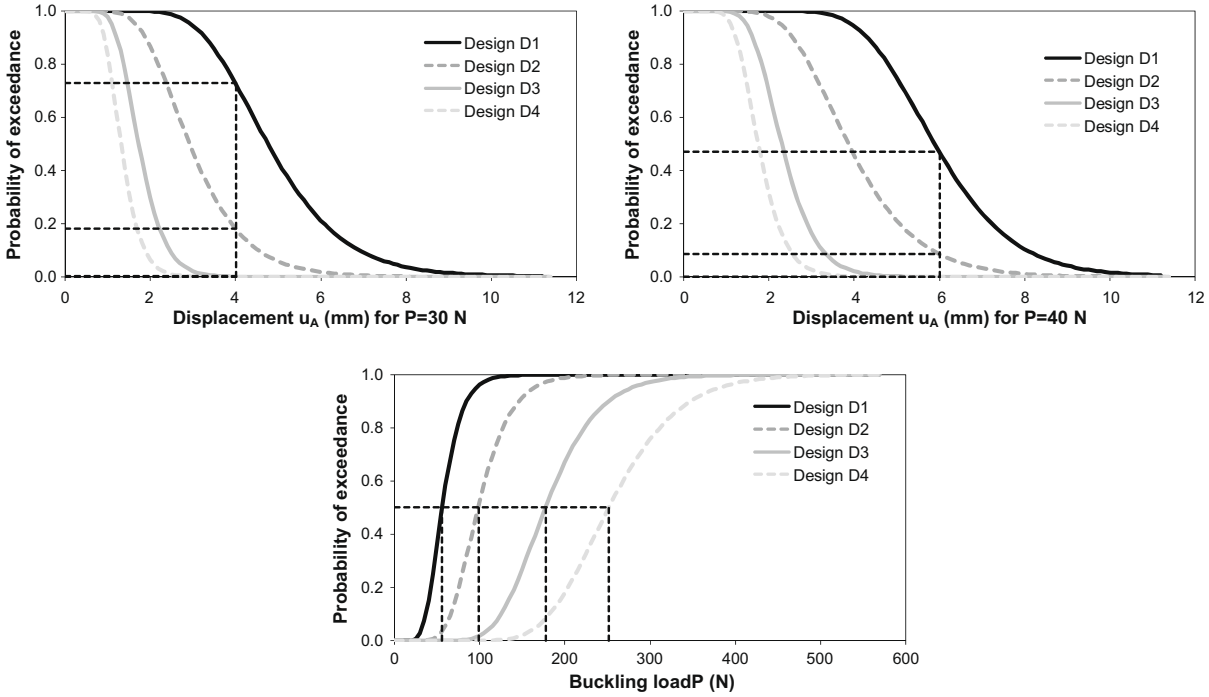

Fig. 9. Fragility curves for the (a) first, (b) second and (c) buckling load limit states.

of variation of the buckling load are given in Table 1. As it can be seen designs D1 and D4 vary significantly, the material volume of D1 is half of that of D4 while the corresponding coefficient of variation of the buckling load is 23% larger.

Fig. 8 presents the histograms of the buckling loads for all aforementioned designs. As it can be seen the mean value of the buckling load and the coefficient of variation varies significantly. The mean value varies from 56.01 N (D1) to 251.97 N (D4), while the coefficient of variation from 32.4% (D1) to 25.2% (D4). Furthermore, the highest buckling load encountered for the D1 is of the order of 150 N (with frequency of occurrence 1 of 1000) while the lowest is of the order of 25 N (with frequency of occurrence 22 of 1000). On the other hand, the highest buckling load encountered for the D4 is of the order of 475 N (with frequency of occurrence 3 of 1000) while the lowest is of the order of 100 N (with frequency of occurrence 2 of 1000). The fragility curves that correspond to the three vulnerability limit states were computed for the four designs and depicted in Fig. 9a–c. As can be seen from these figures, the performance of the four designs D1–D4 vary significantly with reference to the three limit state. From Fig. 9a it can be seen that only designs D3 and D4 satisfy the first vulnerability constraint $P(u_A > 4\ \text{mm}_{|P=30\ \text{N}}) < 5\%$ since for design D2 this probability is equal to 18% while for design D1 it exceeds 70%. In addition, designs D1 and D2 also violate the second vulnerability constraint $P(u_A > 6\ \text{mm}_{|P=40\ \text{N}}) < 3\%$, as it can be seen from Fig. 9b, since for design D2 this probability is equal to 9% while for design D1 it exceeds 45%. Furthermore, design D4 shows the best performance in terms of probability of exceedance of the buckling limit state. As it can be seen from Fig. 9c the 50% probability of exceedance of the buckling limit state is obtained for much different load levels. In particular 55 N for D1, 99 N for D2, 177 N for D3, and 251 N for D4.

Fig. 10 presents the non-linear elastoplastic central load–displacement curves of the perfect structures (no imperfections are incorporated in the non-linear analysis) corresponding to the aforementioned four selected designs while Fig. 11 presents a comparison of the elastic and the elastoplastic load–displacement paths for the two extreme designs D1 and D4. From these figures,

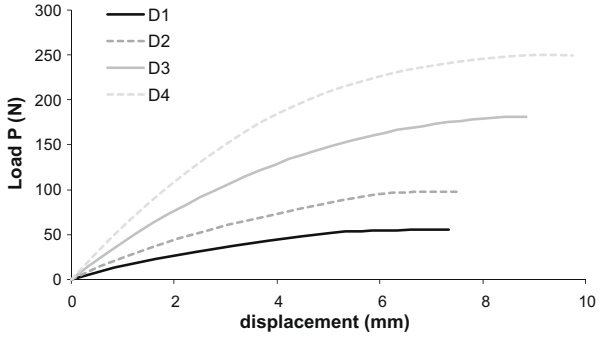

Fig. 10. Central load–displacement curves of the perfect shells corresponding to the D1, D2, D3 and D4 selected designs.

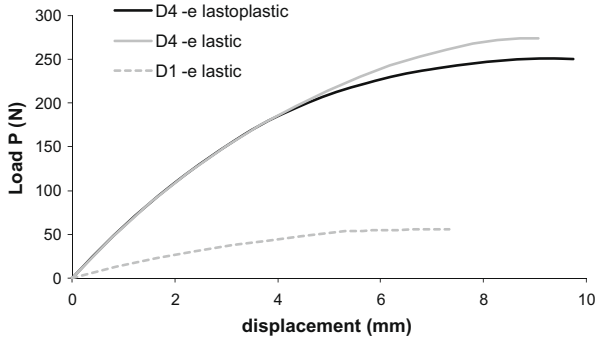

Fig. 11. Comparison of elastic and elastoplastic load–displacement paths for the two extreme designs D1 and D4.

it can be seen that design D1, which corresponds to the optimum with respect to the material volume for the RDO formulation, exhibits purely elastic behaviour up to the limit load. This type of shell appears to be more imperfection sensitive (COV = 32%),

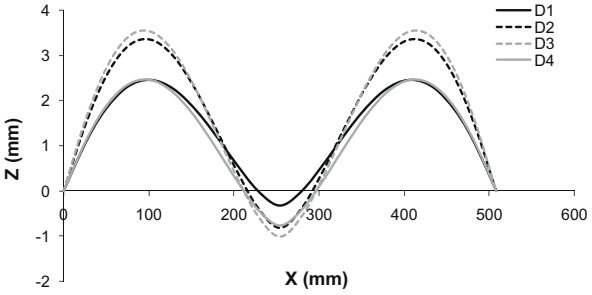

Fig. 12. Deformation patterns at buckling at a cross-section passing through the load point A of the shell (see Fig. 3), corresponding to the D1, D2, D3 and D4 selected designs.

compared to the sensitivity of shell D4 (COV = 25%). On the other hand, D4 shell-type exhibits a more pronounced geometrically non-linear behaviour up to the limit point. Finally, Fig. 12 presents the corresponding deformation patterns of the aforementioned selected designs at buckling, at a cross-section passing through the load point *A* of the shell (see Fig. 1).

6. Conclusions

A design procedure is proposed in the present work that addresses a vulnerability-based robust design optimization (VRDO) of isotropic shell structures possessing uncertain initial geometric as well as material and thickness properties that are modeled as random fields. Two are the main findings of this study:

Incorporating the vulnerability constraints in the context of the optimization problem resulted in significantly different designs compared to the designs obtained with the conventional RDO and RRDO formulations. Furthermore, in all cases examined, the extreme designs composing the multi-objective fronts that fulfill the criteria of the Pareto optimality also differ significantly.

Strength Pareto evolution strategies 2 algorithms are implemented for the solution of the multi-objective optimization algorithm. For the specific problem examined, the improved efficiency of the SPES 2 over the NSES-II algorithm is demonstrated. It seems that for the test cases considered the SPES 2 outperforms the NSES-II since in 15 generations with a population size of 50 members for both parents and offsprings a better quality Pareto front curve is obtained.

References

[1] Schueller GIE. Special issue on computational methods in stochastic mechanics and reliability analysis. Comput Methods Appl Mech Eng 2005;194(12–16):1251–795.
[2] Missoum S, Ramu P, Haftka RT. A convex hull approach for the reliability-based design optimization of nonlinear transient dynamic problems. Comput Methods Appl Mech Eng 2007;196(29–30):2895–906.
[3] Lagaros ND, Papadopoulos V. Optimum design of shell structures with random geometric, material and thickness imperfections. Int J Solids Struct 2006;43(22–23):6948–64.
[4] Allen M, Maute K. Reliability-based shape optimization of structures undergoing fluid–structure interaction phenomena. Comput Methods Appl Mech Eng 2005;194(30–33):3472–95.
[5] Park G-J, Lee T-H, Lee KH, Hwang K-H. Robust design: an overview. AIAA J 2006;44(1):181–91.
[6] Beyer H-G, Sendhoff B. Robust optimization – a comprehensive survey. Comput Methods Appl Mech Eng 2007;196(33–34):3190–218.
[7] Messac A, Ismail-Yahaya A. Multiobjective robust design using physical programming. Struct Multidiscip Optim 2002;23:357–71.
[8] Youn BD, Choi KK, Du L, Gorsich D. Integration of possibility-based optimization and robust design for epistemic uncertainty. J Mech Des, Trans ASME 2007;129(8):876–82.
[9] Tsompanakis Y, Lagaros ND, Papadrakakis M, editors. Structural optimization considering uncertainties. Taylor and Francis, December; 2007. ISBN: 9780415452601.
[10] Papadopoulos V, Papadrakakis M. Finite element analysis of cylindrical panels with random initial imperfections. J Eng Mech, ASCE 2004;130(8):867–76.
[11] Papadopoulos V, Papadrakakis M. The effect of material and thickness imperfections on the buckling load of shells with random initial imperfections. Comput Methods Appl Mech Eng 2005;194(12–16):1405–26.
[12] Noh H-C. Effect of multiple uncertain material properties on statistical behaviour of in-plane and plate structures. Comput Methods Appl Mech Eng 2006;195(19–22):2697–718.
[13] Stefanou G, Papadrakakis M. Stochastic finite element analysis of shells with combined random material and geometric properties. Comput Methods Appl Mech Eng 2004;193(1–2):139–60.
[14] Schenk CA, Schueller GI. Buckling analysis of cylindrical shells with random geometric imperfections. Int J Non-Linear Mech 2003;38:1119–32.
[15] Papadopoulos V, Inglessis P. The effect of non-uniformity of axial loading on the buckling behaviour of shells with random imperfections. Int J Solids Struct 2007;44(18–19):6299–317.
[16] Schenk CA, Schueller GI. Uncertainty assessment of large finite element systems. In: Pfeiffer F, Wriggers P, editors. Lecture notes in applied and computational mechanics. Springer; 2005.
[17] Mourelatos ZP, Liang J. A methodology for trading-off performance and robustness under uncertainty. J Mech Des (ASME) 2006;128:856–63.
[18] Eurocode 3: Design of steel structures, Part 1.1: General rules; Part 1.5: Strength and stability of planar plated structures without transverse loading. European Committee for Standardization; 2004.
[19] Deb K, Pratap A, Agarwal S, Meyarivan T. A fast and elitist multi-objective genetic algorithm: NSGA-II. IEEE Trans Evol Comput 2002;6(2):182–97.
[20] Zitzler E, Laumanns M, Thiele L. SPEA 2: improving the strength Pareto evolutionary algorithm. In: Giannakoglou K, Tsahalis D, Periaux J, Papailou P, Fogarty T, editors. EUROGEN 2001, evolutionary methods for design, optimization and control with applications to industrial problems. Athens, Greece: 2001. p. 95–100.
[21] Schenk CA, Schueller GI. Buckling analysis of cylindrical shells with cutouts including random boundary and geometric imperfections. Comput Methods Appl Mech Eng 2007;196(35–36):3424–34.
[22] Argyris JH, Tenek L, Olofsson L. TRIC, a simple but sophisticated 3node triangular element based on 6 rigid-body and 12 straining modes for fast computational simulations of arbitrary isotropic and laminated composite shells. Comput Methods Appl Mech Eng 1997;145:11–85.
[23] Argyris JH, Tenek L, Papadrakakis M, Apostolopoulou C. Postbuckling performance of the TRIC natural mode triangular element for isotropic and laminated composite shells. Comput Methods Appl Mech Eng 1998;166:211–31.
[24] Argyris JH, Papadrakakis M, Karapitta L. Elastoplastic analysis of shells with the triangular element TRIC. Comput Methods Appl Mech Eng 2002;191(33):3613–37.
[25] Shinozuka M, Deodatis G. Simulation of multi-dimensional Gaussian stochastic fields by spectral representation. Appl Mech Rev ASME 1996;49:29–53.
[26] Coello Coello CA. An updated survey of GA-based multi-objective optimization techniques. ACM Comput Surv 2000;32(2):109–43.
[27] Marler RT, Arora JS. Survey of multi-objective optimization methods for engineering. Struct Multidiscip Optim 2004;26(6):369–95.
[28] Bäck T, Schwefel H-P. An overview of evolutionary algorithms for parameter optimization. J Evol Comput 1993;1(1):1–23.
[29] Lagaros ND, Fragiadakis M, Papadrakakis M. Optimum design of shell structures with stiffening beams. AIAA J 2004;42(1):175–84.